1-2-2024

Innovative Cyanine-Based Fluorescent Dye for Targeted Mitochondrial Imaging and Its Utility in Whole-Brain Visualization

Xin Yan
Michigan Technological University, xyan@mtu.edu

Xinqian Chen
Michigan Technological University, xinqianc@mtu.edu

Zhiying Shan
Michigan Technological University, zhiyings@mtu.edu

Lanrong Bi
Michigan Technological University, lanrong@mtu.edu

Recommended Citation

Yan, X., Chen, X., Shan, Z., & Bi, L. (2024). Innovative Cyanine-Based Fluorescent Dye for Targeted Mitochondrial Imaging and Its Utility in Whole-Brain Visualization. *ACS Omega, 9*(2), 2585-2596.
http://doi.org/10.1021/acsomega.3c07374
Retrieved from: https://digitalcommons.mtu.edu/michigantech-p2/492

Follow this and additional works at: https://digitalcommons.mtu.edu/michigantech-p2

 Part of the Chemistry Commons, and the Kinesiology Commons

ACS OMEGA

Open Access

http://pubs.acs.org/journal/acsodf

Article

Innovative Cyanine-Based Fluorescent Dye for Targeted Mitochondrial Imaging and Its Utility in Whole-Brain Visualization

Xin Yan, Xinqian Chen, Zhiying Shan,* and Lanrong Bi*

Cite This: *ACS Omega* 2024, 9, 2585−2596

Read Online

ACCESS | Metrics & More | Article Recommendations

ABSTRACT: Conducting in vivo brain imaging can be a challenging task due to the complexity of brain tissue and the strict requirements for safe and effective imaging agents. However, a new fluorescent dye called Cy5-PEG2 has been developed that selectively accumulates in mitochondria, enabling the visualization of these essential organelles in various cell lines. This dye is versatile and can be used for the real-time monitoring of mitochondrial dynamics in living cells. Moreover, it can cross the blood−brain barrier, making it a promising tool for noninvasive in vivo brain imaging. Based on the assessment of glial cell responses in the hippocampus and neocortex regions using GFAP and Iba1 biomarkers, Cy5-PEG2 seems to have minimal adverse effects on brain immune response or neuronal health. Therefore, this mitochondria-targeting fluorescent dye has the potential to advance our understanding of mitochondrial dynamics and function within the broader context of whole-brain physiology and disease progression. However, further research is needed to evaluate the safety and efficacy of Cy5-PEG2.

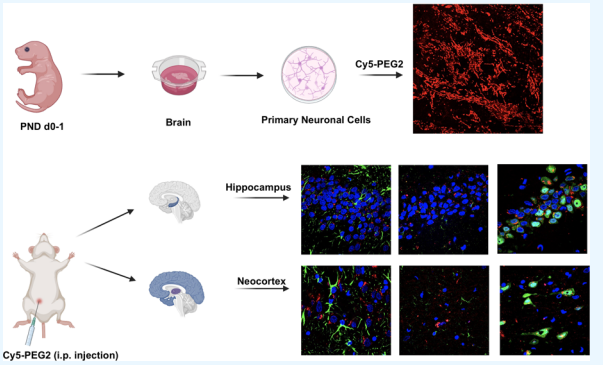

1. INTRODUCTION

Mitochondria-targeting fluorescent dyes can help scientists observe and track changes in mitochondrial health and form in real time, providing vital information about the function and dysfunction of mitochondria in many diseases. This is especially crucial for neurodegenerative diseases, as mitochondrial dysfunction is often an initial symptom.[1,2] Detecting even minor changes in mitochondrial function through noninvasive methods is essential for early detection and effective intervention. Creating specific fluorescent dyes for each disease can also enable personalized diagnosis and treatment approaches tailored to each patient. This will be a significant achievement if successful, since neurodegenerative diseases are typically complex and varied, and personalized approaches are essential for successful treatment.

The use of fluorescent dyes in bioimaging has significantly transformed the field, particularly with the introduction of cyanine derivatives. Cyanine-based fluorescent dyes are designed to emit light when excited by a specific wavelength, making them valuable tools for biological imaging.[3] We are currently focused on expanding the library of these derivatives to develop improved dyes that possess enhanced properties, such as increased brightness and biocompatibility.

It is known that dysfunctional mitochondria are linked to neurodegenerative diseases, and specific changes in these organelles can serve as biomarkers for disease progression.[1,2,4] We strived to develop new mitochondria-targeting fluorescent dyes to help detect and monitor these biomarkers. Previous studies show that the accumulation of amyloid β (Aβ) peptide in the brains of individuals with Alzheimer's disease (AD) significantly contributes to the disease's development and progression.[5,6] It is believed that Aβ accumulation led to mitochondrial dysfunction, further exacerbating neurodegeneration.[5,6]

This manuscript reported the synthesis and biological evaluation of our newly synthesized mitochondria-targeting fluorescent dye, Cy5-PEG2. We conducted biological evaluations of this dye and used it to monitor changes in mitochondrial morphology and dynamics under normal and Alzheimer's disease-like conditions, specifically in the presence of the Aβ_{1-42} peptide. We also investigated the ability of the Cy5-PEG2 dye to penetrate the BBB and be used for in vivo brain imaging.

2. MATERIALS AND METHODS

2.1. Synthesis Procedure. The experiment utilized reagents and solvents obtained from commercial sources and used as received unless otherwise specified. Thin-layer

Received: September 24, 2023
Revised: December 1, 2023
Accepted: December 12, 2023
Published: January 2, 2024

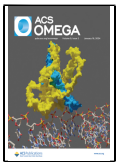

chromatography (TLC) was carried out on Sigma-Aldrich TLC plates, which were silica gel and had a plate number of 1 over the glass support with a thickness of 0.25 μm. Flash column chromatography was performed with Alfa Aesar silica gel, which had a particle size of 230−400 mesh. Melting points were measured by using a MELTEMP melting point apparatus and were uncorrected. The 1H and 13C nuclear magnetic resonance (NMR) spectra were measured by using a Varian UNITY INOVA instrument at 400 and 100 MHz, respectively. The chemical shifts (δ) were reported in reference to solvent residual peaks (dimethyl sulfoxide (DMSO)-d_6, 1H, δ = 2.50 ppm, 13C, δ = 39.52 ppm). The data were reported as follows: chemical shift, multiplicity (s = singlet, d = doublet, t = triplet, q = quartet, and m = multiplet), coupling constant J, and integration. High-resolution mass spectra (HR-MS) were obtained on a JEOL JMS HX 110A mass spectrometer. UV−vis spectra were recorded on a PerkinElmer Lambda 35 UV/vis Spectrometer equipped with a PTP 1 + 1 Peltier Temperature Programmer accessory at 37 °C. Fluorescence spectra were obtained with a Horiba Jobin Yvon Fluoromax-4 spectrofluorometer using an excitation wavelength of 360 nm and slit widths of 5 nm.

*2.1.1. Synthetic Procedure for N-((1E,3E)-3-(Phenylimino) prop-1-en-1-yl)aniline (Compound **1**).* To a stirring solution of distilled water (100 mL), HCl (20 mL), and 1,1,3,3-tetramethoxypropane (10.0 g, 0.11 mol) was added dropwise a combination of distilled water (100 mL), HCl (25 mL), and aniline (15 g, 0.10 mol) and continued stirring for around 50 °C for 3 h. After filtration, the filtrate was further washed with ether to yield compound **1** (8.8 g, 50%) as an orange powder. ^{1}H NMR (400 MHz, DMSO-d_6) 6.53 (t, J = 11.5 Hz, 1H), 7.16 (t, J = 7.2 Hz, 2 H), 7.26−7.62 (m, 8H), 7.16 (t, J = 7.2 Hz, 2H). ^{13}C NMR (101 MHz, DMSO-d_6) δ: 159.00, 139.31, 130.42, 126.44, 118.04, 99.34.

*2.1.2. Synthetic Procedure for 2,3,3-Trimethyl-3H-indole (Compound **2**).* To a stirring solution of phenylhydrazine (3.24 g, 0.03 mol) and glacial acetic acid (25 mL) was added 3-methylbutanone (5 mL, 0.035 mol). Then, the mixture was kept refluxed at 118 °C. The mixture was subjected to evaporation using a rotary evaporator, and the resulting residue was separated using 50 mL of ether and 50 mL of water. The water layer was rewashed with ether. The combined organic layers were then evaporated until they dried out, resulting in a yield of 4.0 g of compound **2** (83%), which was a brownish liquid. ^{1}H NMR (400 MHz, $CDCl_3$) δ ppm 1.26 (s, 6H), 2.24 (s, 3H), 7.15 (t, J = 7.4 Hz, 1H), 7.25 (dd, J = 8.9, 4.1 Hz, 2H), 7.51 (d, J = 7.6 Hz, 1H). ^{13}C NMR (101 MHz, $CDCl_3$) δ: 188.17, 153.56, 145.69, 127.74, 125.30, 121.45, 119.99, 119.68, 53.84, 23.37, 15.62.

*2.1.3. Synthetic Procedure for 1-Ethyl-2,3,3-trimethyl-3H-indol-1-ium (Compound **3**).* To synthesize 1-ethyl-2,3,3-trimethyl-3*H*-indol-1-ium, an SN2 reaction was proceeded between 2,3,3-trimethyl-3*H*-indole and ethyl iodide in the presence of acetonitrile as the solvent. To create a homogeneous reaction mixture, the first step involves dissolving 2,3,3-trimethyl-3*H*-indole in acetonitrile. Next, the deprotonated nitrogen atom in 2,3,3-trimethyl-3*H*-indole acts as a nucleophile and attacks the carbon atom in ethyl iodide, forming a new carbon−nitrogen bond. The iodide ion is displaced as a leaving group, and the rearrangement of the molecule stabilizes the positive charge on the nitrogen atom.

4.0 g of compound **2** was dissolved in 50 mL of acetonitrile, and 5 mL of ethyl iodide was added. The mixture was then refluxed under nitrogen protection for 48 h. After evaporation with a rotatory evaporator, the crude residue was washed with ether to obtain compound **3** as an orange powder, with a yield of 4.2 g (89%). ^{1}H NMR (400 MHz, $CDCl_3$) δ (ppm): 1.54−1.58 (m, 9H), 3.06 (s, 3H), 4.66 (m, 2H), 7.51 (m, 3H), 7.54 (m, 1H).

*2.1.4. Synthetic Procedure for 1-(5-Carboxypentyl)-2,3,3-trimethyl-3H-indol-1-ium (Compound **4**).* To a stirring solution of potassium iodide (3.70 g, 22 mmol) in 30 mL of acetonitrile was added 6-bromohexanoic acid (2.0 g, 10 mmol) dropwise and kept stirring at 50 °C. After gently heating for 0.5 h, 2,3,3-trimethyl-3*H*-indole (1.6 g, 10 mmol) was added, and the mixture was refluxed overnight. After the mixture was cooled to room temperature, the crude residue was washed with dichloromethane and concentrated with a rotary evaporator. The obtained residue was then washed with ether to yield compound **4** (3.12 g, 78%) as a gray solid. ^{1}H NMR (400 MHz, DMSO-d_6) δ ppm 1.37 (d, J = 17.5 Hz, 2H), 1.51 (m, 6H), 1.82 (p, J = 7.9 Hz, 2H), 2.19 (q, J = 6.7, 6.1 Hz, 2H), 2.47 (td, J = 3.3, 2.8, 1.4 Hz, 2H), 2.82 (s, 3H), 4.43 (t, J = 7.7 Hz, 2H), 7.56−7.64 (m, 2H), 7.73−7.89 (m, 1H), 8.90−8.00 (m, 1H).

*2.1.5. Synthetic Procedure for Compound **5**.* To a stirring solution of compound **3** (1 g, 3.2 mmol) in acetic acid and acetic anhydride, compound **1** (1 g, 3.8 mmol) was added and refluxed under N_2 for 1 h. After cooling to room temperature, a solution of compound **4** (2.0 g, 5 mmol) in anhydrous pyridine was added to the mixture and continued stirring under N_2 at room temperature overnight. After precipitation with cold ether, the green solution was decanted, leaving crude compound **5** (∼3.2 mmol) as a green solid directly used for the next steps.

*2.1.6. Synthetic Procedure for Compound **6**.* To a stirring solution of crude compound **5** (∼3.2 mmol) in 50 mL of dichloromethane were sequentially added 2-(2-(but-3-yn-1-yloxy) ethoxy)ethan-1-amine (0.62 mL, 4.3 mmol), 2-(1*H*-benzotriazol-1-yl)-1, (1,3,3-tetramethyluronium-hexafluorophosphate, HBTU) (2.0 g 5 mmol), and 5 mL of triethylamine. The mixture was gently stirred overnight. After evaporating the solvent with a rotary evaporator, the crude residue was further purified via flash chromatography on silica gel (eluent/DCM/MeOH = 40:1) to yield compound **6** as a green solid. ^{1}H NMR (500 MHz, CDCl3) δ ppm 1.36−1.38(m, 3H), 1.42−1.44(m, 2H), 1.64−1.66(m, 14H), 1.66−1.74(m, 2H), 2.15 (t, J = 7.5 Hz, 2H), 2.37 (t, J = 2.5 Hz, 1H), 3.31−3.34 (m, 2H), 3.44−3.46(m, 2H), 3.52−3.62(m, 4H), 3.87−4.21(m, 4H), 6.02−6.09(m, 2H) 6.35 (t, J = 2.5 Hz, 1H), 6.55(t, J = 15 Hz, 1H), 7.01−7.05(m, 2H), 7.09−7.15(m, 2H), 7.24−7.28(m, 4H), 7.87 (td, J = 4, 2.8, 1.4 Hz, 2H):^{13}C NMR (101 MHz, DMSO-d_6) δ 173.08, 172.91, 172.67, 165.65, 153.40, 153.23, 141.90, 141.51, 141.36, 141.22, 128.65, 128.63, 125.79, 125.21, 125.14, 122.29, 122.23, 110.57, 110.41, 103.20, 103.06, 79.62, 77.56, 77.31, 77.05, 74.79, 69.90, 69.52, 69.05, 58.29, 49.39, 49.33, 44.01, 39.13, 39.00, 38.55, 35.98, 27.78, 27.68, 27.00, 26.32, 25.13, 12.22.

2.2. Cell Culture. HEK293 cells were purchased from the American Type Culture Collection (ATCC). The HEK293 cells were cultured in Dulbecco's modified Eagle's medium (DMEM), supplemented with fetal bovine serum (FBS), to attain a final concentration of 10%. Growth media were replaced every 2−3 days.

Human umbilical vein endothelial cells (HUVECs) were purchased from the ATCC. The HUVECs were then cultured

https://doi.org/10.1021/acsomega.3c07374
ACS Omega 2024, 9, 2585−2596

in Dulbecco's modified Eagle's medium (DMEM), which was supplemented with 5.5 mM glucose, 10% fetal bovine serum (FBS), 100 U/mL penicillin, and 100 mg/mL streptomycin. They were kept at 37 °C in a 5% CO_2-humidified incubator to maintain the cells.

HeLa cells were purchased from the ATCC. To maintain them for the imaging study, RPMI-1640 medium was used, and then 10% fetal bovine serum, 2 mM glutamine, 100 μg/mL penicillin, and streptomycin were added. The cells were kept in a humid atmosphere with 5% CO_2 at 37 °C.

2.3. Subcellular Localization Study of Cy5-PEG2 Dye. To cultivate cells on coverslips, they are placed in a Petri dish filled with the culture medium. Once the cells have reached the desired density, the medium is removed from the dish and a prewarmed (37 °C) staining solution is added that comprises a MitoTracker (1 μM)/LysoTracker probe (1 μM), Cy5-PEG2 dye (1 μM), and Hoechst 33342 (1 μg/mL). After incubating the cells for 30 min, the staining solution is replaced with fresh, prewarmed media. Finally, we examined the cells using a confocal laser scanning fluorescence microscope. To analyze the obtained images, ImageJ analysis software was used. The colocalization of the fluorescent signals from the dyes is quantified using a MitoTracker/LysoTracker probe and the Cy5-PEG2 dye. This provides information about the location of the Cy5-PEG2 dye within the cells.

2.3.1. Animals. Adult Sprague−Dawley (SD) rats used in this study were purchased from Charles River Laboratories (Wilmington, MA). All animals were obtained on a 12:12 h light−dark cycle in a climate-controlled room, and chow and water were provided ad libitum. This study was carried out in strict accordance with the recommendations in the Guide for the Care and Use of Laboratory Animals of the National Institutes of Health. The protocol was approved by the Michigan Technological University Institutional Animal Care and Use Committee.

2.4. Primary Neuronal Cell Culture. The primary neuronal cells were isolated from the brain tissues of 1−3 day old SD pups using the papain dissociation system as instructed by the manufacturer. These neurons were then cultured in neurobasal-A medium supplemented with 2% B27+ and 1% antibiotic-penicillin/streptomycin on poly(D-lysine)-coated 35 mm dishes. The cells were incubated at 37 °C in an incubator containing 5% CO_2, and the medium was replaced every 3 days. After 7−10 days, the neuronal cultures were incubated with Aβ1−42 peptide at varying concentrations for 24 h and then costained with the Cy5-PEG2 dye (1 μM, green fluorescence) and Hoechst (0.1 μg/mL, blue) for the study of mitochondrial morphology and dynamics.

2.5. Intraperitoneal (i.p.) Injection of the Cy5-PEG2 Dye into SD Rats. To examine the potential of Cy5-PEG2 to penetrate the blood−brain barrier (BBB) in rats, several steps are involved in the intraperitoneal (ip) injection of Cy5-PEG2 into SD rats. Ensuring that all instruments and materials are sterile before proceeding is crucial. A working solution of Cy5-PEG2 in sterile PBS is prepared based on the manufacturer's instructions. SD rats are anesthetized with 5% isoflurane, and the depth of anesthesia is monitored to prevent unnecessary suffering. The anesthetized rats are positioned on a clean surface, and the Cy5-PEG2 solution (200 nM) is injected intraperitoneally using a sterile syringe and needle. After the injection, the rats recovered from anesthesia on a heating pad or under a heat lamp. The rats are closely monitored during the recovery period. After 24 h of post injection, the rats are euthanized using 5% isoflurane, and then transcardial perfusion is performed with PBS to remove residual blood from the circulatory system. The brains are extracted, the brain tissue is fixed, and the tissue sections are prepared for analysis. The brain tissue slides are then subjected to confocal fluorescent microscopy imaging. The penetration of Cy5-PEG2 into the brain tissues is assessed, and appropriate controls, including animals treated with a vehicle only, are included in the experiment. Fluorescence intensity in the brain regions is quantified and compared using ImageJ.

3. RESULTS

3.1. Rationale of Molecular Design. Asymmetric cyanine dyes are highly favored over symmetric ones for several reasons.[3,7] They produce brighter, more sensitive signals and better absorption and emission characteristics. Their longer wavelengths make them less susceptible to background interference and improve light penetration into biological samples. Furthermore, asymmetric cyanine dyes have large Stokes shifts, which reduces background noise and enhances discrimination between excitation and emission lights.[3,7] As a result, we have developed a series of new fluorescent dyes, such as Cy5-PEG2, based on the asymmetric cyanine structure.

The molecular design of Cy5-PEG2 incorporates both the PEG linker and the terminal alkyne group for specific reasons related to brain imaging, particularly in targeting the mitochondria of brain cells and crossing the blood−brain barrier (BBB).

The terminal alkyne group serves as a bioorthogonal handle for click chemistry reactions, specifically copper-catalyzed azide−alkyne cycloaddition (CuAAC), allowing for the selective and efficient labeling of biomolecules in complex biological systems. The alkyne functional group enables modularity in synthesizing imaging agents, providing a specific site for attaching ligands or targeting moieties and enhancing the probe's ability to interact with biological targets in the brain. The relatively small size of the alkyne group reduces steric hindrance, making it advantageous for the probe to navigate through the complex structure of the BBB, which is crucial for enhancing penetration of the imaging agent into the brain parenchyma.

The presence of PEG increases the water solubility and biocompatibility of the imaging probe, ensuring that it can circulate effectively in the bloodstream without causing adverse effects. PEGylation improves the pharmacokinetics of the molecule by reducing the potential clearance and increasing the circulation time, allowing the imaging agent to reach its target site within the brain. PEGylation plays a crucial role in enhancing the ability of drug delivery systems to target mitochondria.[8] In the context of brain imaging, effective penetration into brain cells includes mitochondria. Studies have shown that PEGylation increases hydrophilicity, reduces nonspecific interactions with cell membranes, and improves cellular uptake.

The asymmetric cyanine derivative with a PEG linker enhances cellular uptake, protects the fluorescent dye from degradation, and improves the mitochondria-targeting capacity, making it suitable for imaging applications focusing on visualizing mitochondria in brain cells. The emission of cyanine derivatives, such as Cy5, in the near-infrared (NIR) range reduces tissue autofluorescence and allows for deeper tissue penetration, making them ideal for in vivo imaging.

https://doi.org/10.1021/acsomega.3c07374
ACS Omega 2024, 9, 2585−2596

Scheme 1. Synthetic Scheme of Preparation of the Cy5-PEG2 Dye

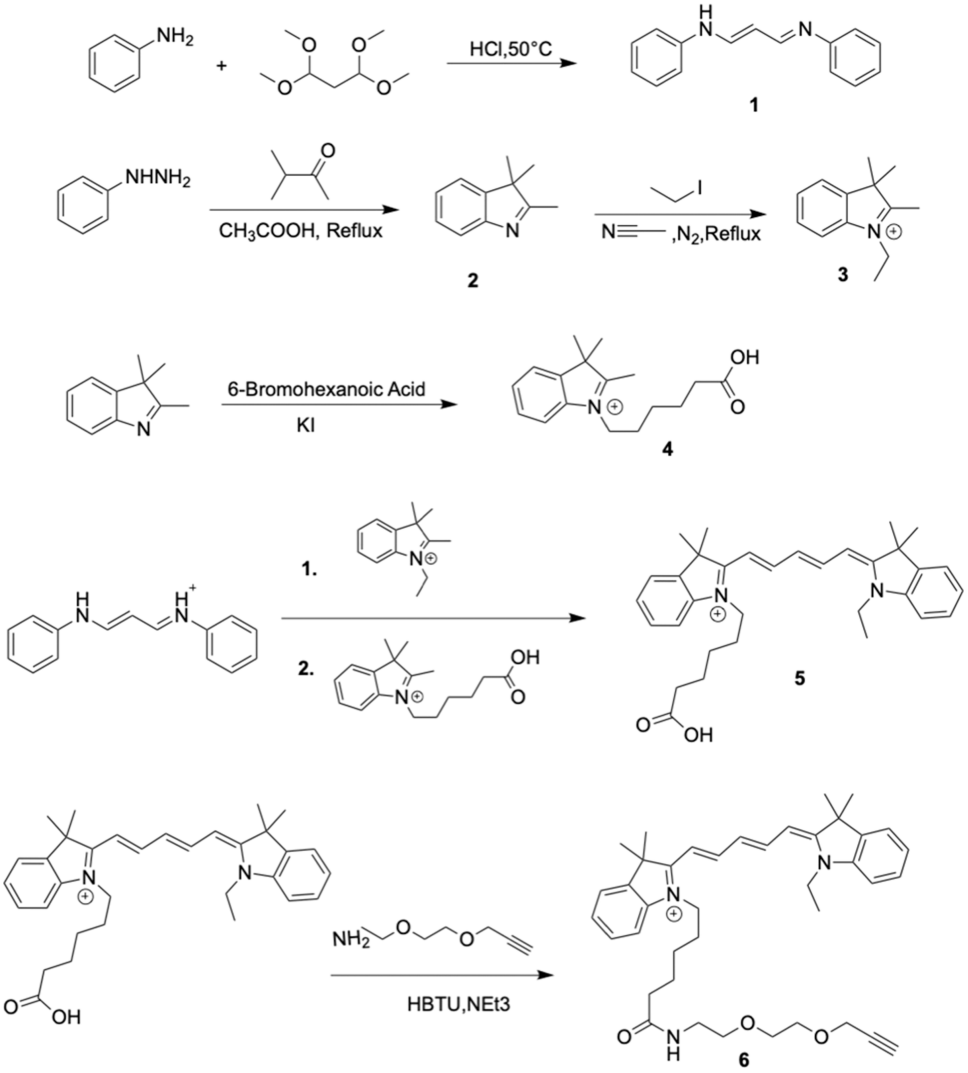

The molecular design of Cy5-PEG2 with the terminal alkyne group and PEG linker is strategically chosen to leverage click chemistry for functionalization, enhance BBB penetration, ensure biocompatibility, improve pharmacokinetics, and specifically target mitochondria within brain cells for practical brain imaging applications.

3.2. Synthesis of the Cy5-PEG2 Dye. Using HCl, 1,1,3,3-tetramethoxypropane (TMP), and aniline to create compound **1**, this reaction involves the formation of an iminium ion intermediate, followed by an intramolecular cyclization reaction and a rearrangement and deprotonation step. Using phenylhydrazine, glacial acetic acid, and 3-methylbutanone to prepare compound **2**, this process involves forming phenylhydrazine acetate followed by adding phenylhydrazine acetate to 3-methylbutanone to form an imine intermediate, which then undergoes protonation and rearrangement to form a more stable enamine intermediate. The enamine intermediate subsequently undergoes intramolecular cyclization, resulting in the formation of compound **2**. To create compound **3**, an SN2 reaction between compound 2 and ethyl iodide is necessary while using acetonitrile as the solvent. In this reaction, the deprotonated nitrogen atom in compound **2** acts as a nucleophile to attack the carbon atom in ethyl iodide, forming a new carbon−nitrogen bond. Then, the iodide ion is displaced as a leaving group, and the rearrangement of the molecule stabilizes the positive charge on the nitrogen atom. The synthesis of compound **4** also involves a multistep reaction mechanism. In this process, a potassium bromide salt is first formed and then reacts with an acyl iodide intermediate through a nucleophilic substitution reaction between 6-bromohexanoic acid and potassium iodide. The second step is a nucleophilic addition reaction between the acyl iodide and 2,3,3-trimethyl-3*H*-indole, forming a tetrahedral intermediate. The third step involves the rearrangement of the tetrahedral intermediate to a zwitterionic intermediate, followed by the elimination of a proton to form the desired product. Asymmetric cyanine dye **5** was synthesized using a known condensation reaction of carboxyindoleninium salt **4**, compound **3**, and malonaldehyde dianil **1**. This process involves incorporating the quaternary ammonium group into the cyanine core and subsequent alkylation of the tertiary amino group. Finally, compound **5** proceeded with the coupling reaction with a PEG linker to provide the Cy5-PEG2 dye **6** (Scheme 1).

When considering a new fluorescent dye for monitoring changes in mitochondrial morphology and dynamics during cellular assays, assessing a few critical factors is essential. One crucial aspect is the dye's ability to accumulate selectively in

https://doi.org/10.1021/acsomega.3c07374
ACS Omega 2024, 9, 2585−2596

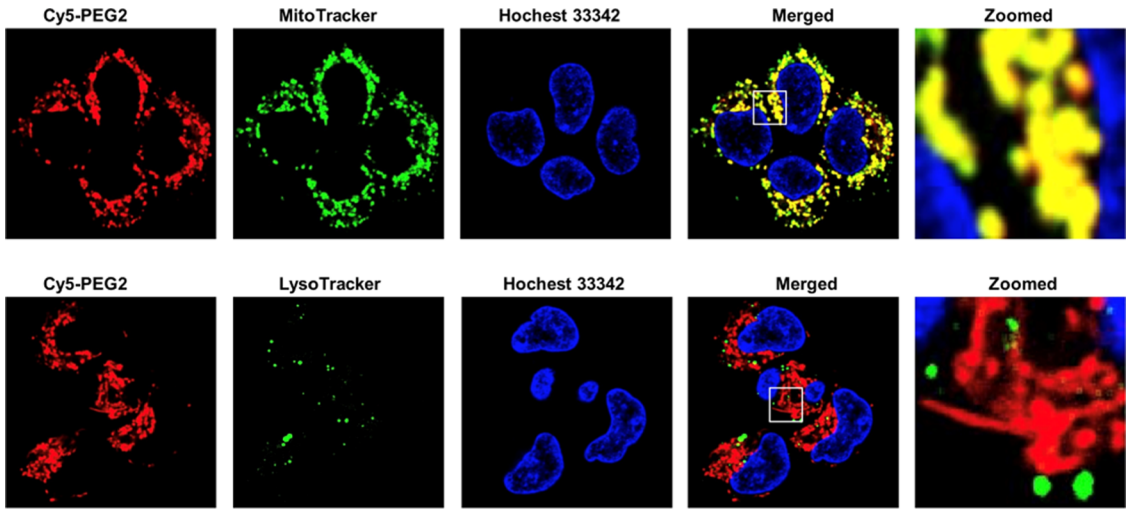

Figure 1. Intracellular distribution of the Cy5-PEG2 dye compared to those of MitoTracker and LysoTracker. HEK293 cells incubated with the Cy5-PEG2 dye (1 μM, red fluorescence), followed by counterstaining with MitoTracker (1 μM, row 1)/LysoTracker (1 μM, green fluorescence, row 2), Hoechst 33342 (1 μg/mL, blue fluorescence) for 30 min; the images were taken at randomly selected areas to ensure the imaging conditions were consistent throughout the experiments. The experiments were repeated four times to ensure the reliability of the results. Cells were imaged on an inverted laser scanning fluorescent microscope (Olympus) using a 60 × oil immersion objective lens.

mitochondria while reducing its binding to other cellular components. This ensures the precise labeling of mitochondria and specificity for this organelle. Additionally, the dye should penetrate cell and mitochondrial membranes without causing toxicity or interfering with mitochondrial function. An optimal fluorescent dye for live-cell imaging should be photostable, exhibit high fluorescence brightness, and contrast against the cellular background. Lastly, it is vital to evaluate the dye's compatibility with the specific experimental conditions of the cellular assays. Herein, we conducted various assays to determine whether the Cy5-PEG2 dye suits live-cell imaging assays.

3.3. Mitochondrial Targeting Property of the Cy5-PEG2 Dye. First, we examine the subcellular localization of Cy5-PEG2 dye in HEK293 cells derived from human embryonic kidney cells and commonly used in cell biology research for various applications. HEK293 cells are a popular choice because they are easy to culture and grow quickly and their relatively large size and flat morphology make them suitable for cell imaging.

We performed a cellular imaging experiment using a confocal laser scanning fluorescent microscope and Cy5-PEG2 dye at a concentration of 1 μM. The dye was incubated for 30 min, producing bright fluorescence and fast cellular internalization (Figure 1). Furthermore, the Cy5-PEG2 dye showed remarkable photostability, allowing us to carry out prolonged confocal imaging without considerable photobleaching on HEK293 cells.

When conducting colocalization studies, we examine the spatial overlap of two molecules within a cell. Our present study looks at the colocalization of Cy5-PEG2 dye and MitoTracker, a probe commonly used to label mitochondria. We acquired fluorescent images of the samples using a confocal laser scanning microscope system. To ensure the accuracy of our results, we used ImageJ image analysis software to analyze the acquired images. Our analysis allowed us to determine the extent to which the two fluorescent signals overlapped. We used Pearson's colocalization coefficient (PCC) to quantify this overlap, which calculates coefficients or pixel intensities that indicate the degree of overlap between the two signals. The fluorescence image produced using Cy5-PEG2 dye exhibits high levels of colocalization with that of MitoTracker [Pearson's correlation coefficient (PCC_{HEK293}): 0.90 in HEK293 cells]. The observed high Pearson's correlation coefficient established the mitochondrial specificity of the two probes. To further confirm the organelle-specificity of the Cy5-PEG2 dye, we stain the cells with Lysotracker, which explicitly labels lysosomes. Our observation that the Cy5-PEG2 dye overlaps with MitoTracker but not with Lysotracker suggests that the Cy5-PEG2 dye specifically stains mitochondria and not lysosomes (Figure 1).

To further examine the fluorescent dyes' subcellular localization, it is beneficial to use different cell lines. By examining the performance of the Cy5-PEG2 dye in different cell types, we can determine whether the observed localization is consistent across various cellular environments or specific to a particular cell line. We compared the localization patterns across different cell types (HUVEC, HEK293, and HeLa cell lines) and noted similarities (data not shown). We further performed statistical analysis to quantify and compare the localization patterns quantitatively. This analysis involved calculating colocalization coefficients (PCC_{HUVEC}: 0.88 and PCC_{HeLa}: 0.92) and measuring signal intensity. We finally confirmed that the subcellular localization of Cy5-PEG2 dye is consistent across the tested cell types (HUVEC, HEK293, and HeLa cell lines). We then repeated the experiments by using multiple replicates to ensure the reliability of our results. These results could provide solid evidence to support the observed subcellular localization pattern of the Cy5-PEG2 dye observed.

By observing changes in the distribution of the Cy5-PEG2 dye within cells over time, we can capture the dynamic processes within cells. This method helps us validate our initial observations by examining whether the observed localizations remain consistent or change over time. We treated HEK293 cells with the Cy5-PEG2 dye at the predetermined concentration (1 μM) and incubation time (1, 12, 24, and 48 h). We then imaged the cells using a confocal fluorescence microscope at each time point (Figures 2 and 3). We captured

https://doi.org/10.1021/acsomega.3c07374
ACS Omega 2024, 9, 2585−2596

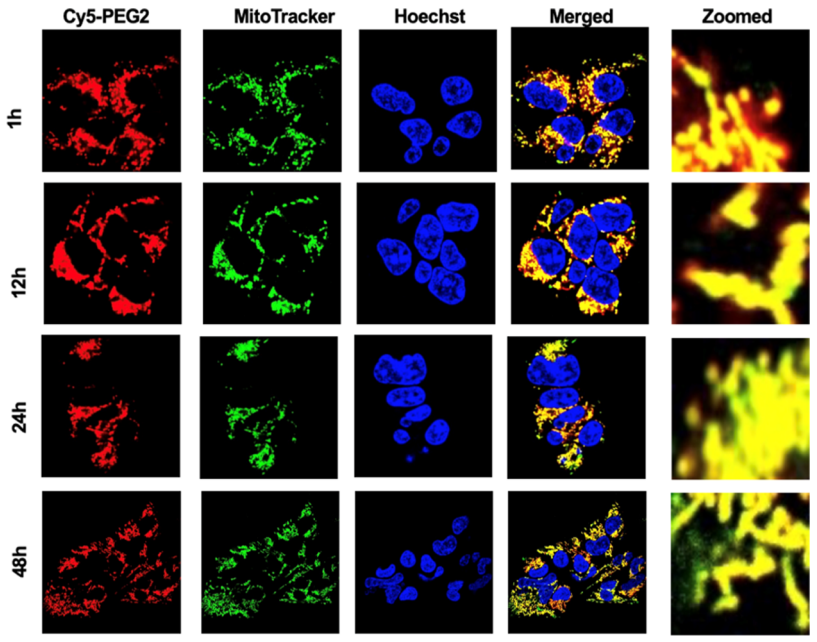

Figure 2. Representative confocal images of the HEK293 cells were taken at different time points (1, 12, 24, and 48 h). The cells underwent a time-course study and were stained with the Cy5-PEG2 dye (1 μM, red fluorescence) and costained with MitoTracker (1 μM, green fluorescence) and Hoechst (1 μg/mL, blue fluorescence). The images were taken at randomly selected areas to ensure the imaging conditions were consistent throughout the experiments. The experiments were repeated four times to ensure the reliability of the results. Cells were imaged on an inverted laser scanning fluorescent microscope (Olympus) using a 60 × oil immersion objective lens.

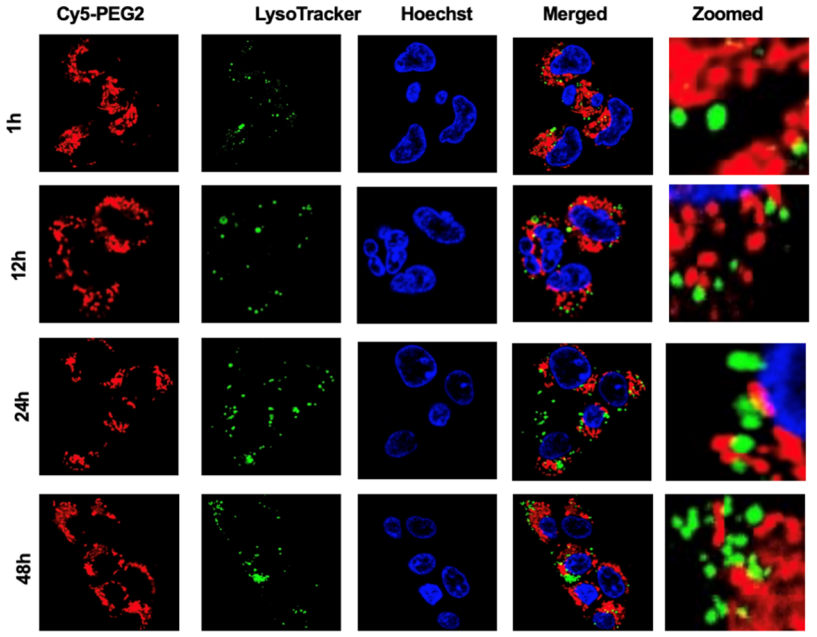

Figure 3. Representative confocal images of the HEK293 cells were taken at different time points (1, 12, 24, and 48 h). The cells underwent a time-course study and were stained with Cy5-PEG2 (1 μM, red fluorescence) and costained with LysoTracker (1 μM, green fluorescence) and Hoechst (1 μg/mL, blue fluorescence). The images were taken at randomly selected areas to ensure the imaging conditions were consistent throughout the experiments. The experiments were repeated four times to ensure the reliability of the results. Cells were imaged on an inverted laser scanning fluorescent microscope (Olympus) using a 60 × oil immersion objective lens.

images of randomly selected areas. We ensured consistent imaging conditions throughout the experiment. We analyzed the acquired images using ImageJ analysis software and found no significant changes in the fluorescent intensity and subcellular localization after incubation with the Cy5-PEG2 dye for an extended time. This indicates that this dye did not affect mitochondrial function or cellular processes over time.

3.4. Cy5-PEG2 Dye Can Effectively Detect Mitochondrial Morphology and Dynamics. Aβ_{1-42} peptide induces mitochondrial dysfunction and impacts mitochondrial morphology and dynamics.[6] Herein, it is crucial to determine whether the newly synthesized Cy5-PEG2 dye can effectively detect these changes. This requires additional experiments to

https://doi.org/10.1021/acsomega.3c07374
ACS Omega 2024, 9, 2585−2596

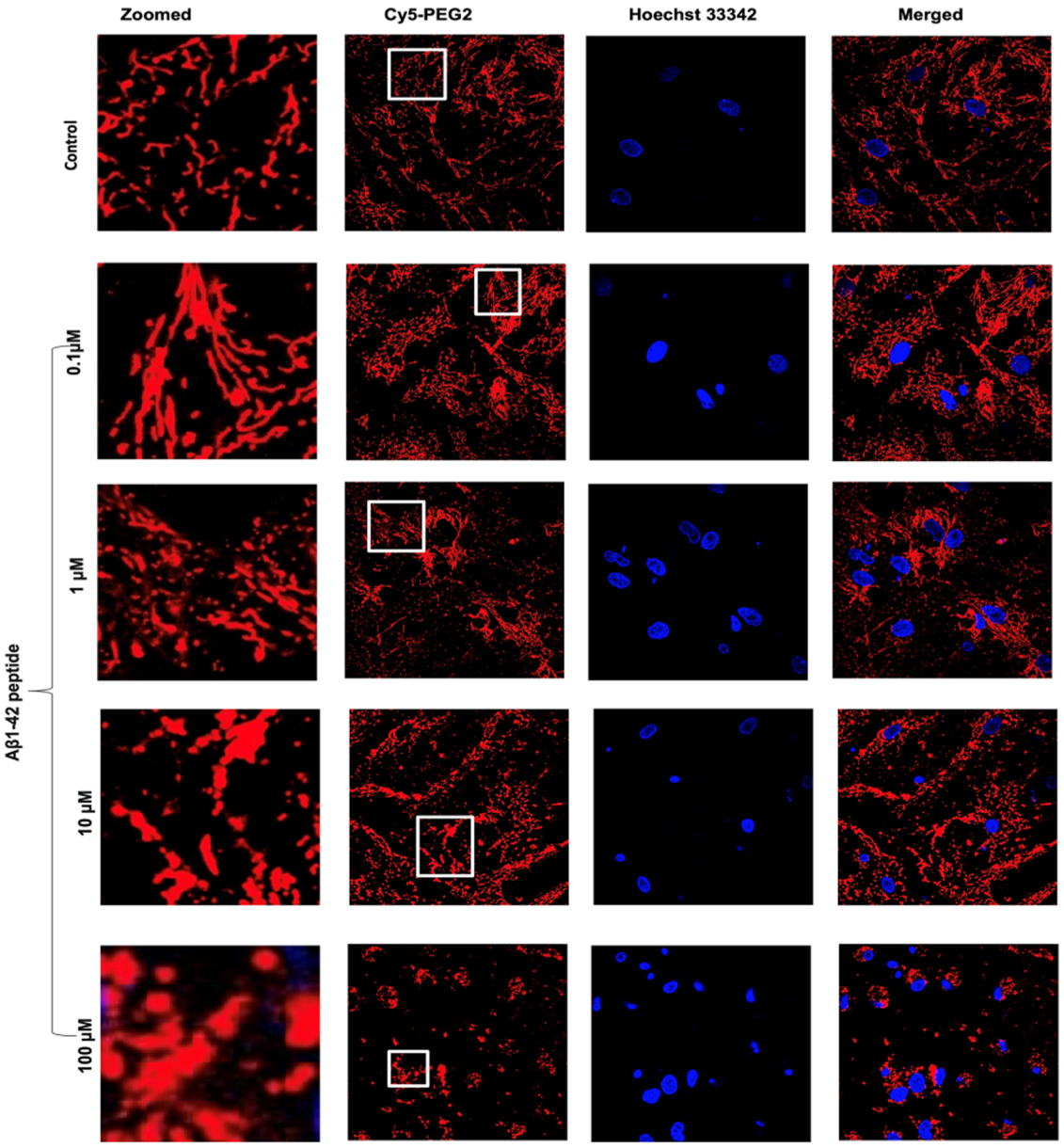

Figure 4. Representative confocal images of the primary neuronal cell lines in the presence of the Aβ_{1-42} peptide at varying concentrations (0, 0.1, 1, 10, and 100 μM) for 24 h. Cells were stained with Cy5-PEG2 (1 μM, red fluorescence) and costained with Hoechst (1 μg/mL, blue fluorescence). The images were taken at randomly selected areas to ensure the imaging conditions were consistent throughout the experiments. The experiments were repeated four times to ensure the reliability of the results. The fluorescent images were obtained with a confocal laser scanning fluorescent microscope using a 60 × objective lens.

evaluate the dye's performance in cells treated with Aβ_{1-42} peptide and compare the results with control cells.

MitoTracker is known to accumulate in active mitochondria due to its negative membrane potential. However, the cell membranes of neuronal cells, particularly primary ones, are more complex and robust compared to those of other cell types. This can affect the penetration ability of MitoTracker through the cell membrane, as it depends on the specific membrane properties of the cell. Additionally, primary neurons may have a mitochondrial membrane potential lower than that of other cell types, making it difficult for MitoTracker to accumulate within the mitochondria. Considering these factors, we chose to use the Cy5-PEG2 dye alone without incorporating MitoTracker for the primary neuronal cell assays that we conducted.

Primary neuronal cells were incubated with Aβ_{1-42} peptide at concentrations ranging from 0.1, 1, 10, and 100 μM for 24 h. At concentrations of 100 μM, most of the mitochondria in primary neuronal cells were fragmented after being incubated with Aβ_{1-42} peptide for 24 h. The cause of this fragmentation is likely due to the Aβ_{1-42} peptide-induced mitochondrial fission, which results in smaller organelles. This disintegration is likely due to mitochondrial fission triggered by the high Aβ_{1-42} peptide concentration. The increased fission disrupts mitochondrial function, leading to cellular malfunction, and may play a role in neurodegenerative processes.[6] However, an interesting phenomenon was observed in cells pretreated with the Aβ_{1-42} peptide at a low concentration (0.1 μM). The mitochondria in low concentrations of Aβ_{1-42} peptide-pretreated cells appeared to have more tubular structures

https://doi.org/10.1021/acsomega.3c07374
ACS Omega 2024, 9, 2585−2596

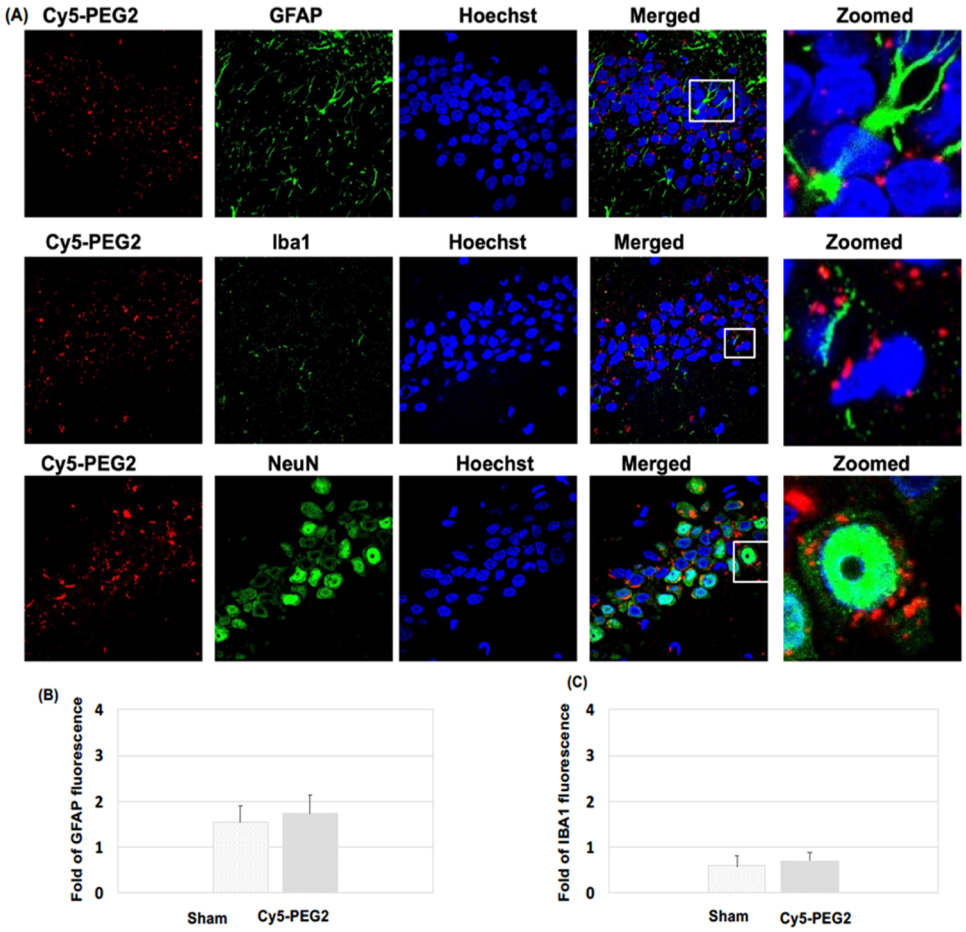

Figure 5. Visualization of the Cy5-PEG2 dye in the hippocampus regions: (A) representative confocal laser scanning images of rat brain sections fixed with 4% PFA. For the entire figure, the red channels represent the fluorescent dye Cy5-PEG2; the green channel represents GFAP- (row I), Iba1- (row II), and NeuN-positive (row III) cells in the brain sections. Zoomed-in pictures are shown on the right. The fluorescent images were obtained with a confocal laser scanning fluorescent microscope using a 60 × objective lens. (B) Quantitative analysis of the fluorescence intensity of GFAP. (C) Quantitative analysis of the fluorescence intensity of IBA1.

and were more interconnected (Figure 4). This could be due to an adaptive response of cells triggered by low concentrations of the Aβ_{1-42} peptide, which helps maintain mitochondrial dynamics and protect cell viability.

3.5. Administering Cy5-PEG2 Dye Intraperitoneally in SD Rats Enables Efficient Traversal of the BBB, Allowing Imaging of Mitochondria in Brain Cells. To determine if the Cy5-PEG2 dye is suitable for brain imaging, it is necessary to test its ability to cross the BBB when an intraperitoneal injection is administered. The BBB is a selective barrier that prevents many therapeutic and imaging agents, including fluorescent dyes, from entering the brain. Administering the dye intraperitoneally allowed us to evaluate its ability to reach the brain from the bloodstream. If the dye can cross the BBB and accumulate in brain tissues, it suggests that it has potential for use in brain imaging. We recently confirmed that the Cy5-PEG2 dye can penetrate the BBB.

As AD progresses, it affects various brain regions, leading to a decline in cognitive abilities and memory loss. The hippocampus is crucial for forming and consolidating memories, but the accumulation of Aβ peptide in this area can impair memory and the ability to create new memories.[9] The neocortex, which includes the frontal, parietal, temporal, and occipital lobes, is also heavily affected by Aβ buildup, resulting in cognitive decline, language difficulties, and problems with executive functions.[9] In our present study, we observed the uptake and distribution of the Cy5-PEG2 dye in these regions. We found that the red fluorescence of the Cy5-PEG2 dye was visible in both the hippocampus and neocortex, indicating that cells, such as neurons and glial cells, in these regions had absorbed this dye.

It is worth mentioning that, after 24 h of injection (i.p.), the intensities of the Cy5-PEG2 red staining are relatively weak. More recently, we conducted biodistribution studies of Cy5-PEG2 and observed that the staining intensity of Cy5-PEG2 gradually decreased over time (data not shown). This decrease could be due to various factors such as the metabolism or clearance of Cy5-PEG2 from the brain tissue over time. The concentration of Cy5-PEG2 in the brain could decrease due to metabolic processes or clearance mechanisms, leading to weaker staining after 24 h.

The initial intense staining at 2 h could be attributed to the efficient binding and uptake of Cy5-PEG2 by the target cells in the brain. However, the binding may become reversible over time, causing the dye to be released from the cells and resulting in weaker staining. Furthermore, the distribution of Cy5-PEG2 within the brain tissue may also change over time, leading to variations in staining intensity in different brain regions. Another contributing factor could be that the Cy5-PEG2 dye

https://doi.org/10.1021/acsomega.3c07374
ACS Omega 2024, 9, 2585−2596

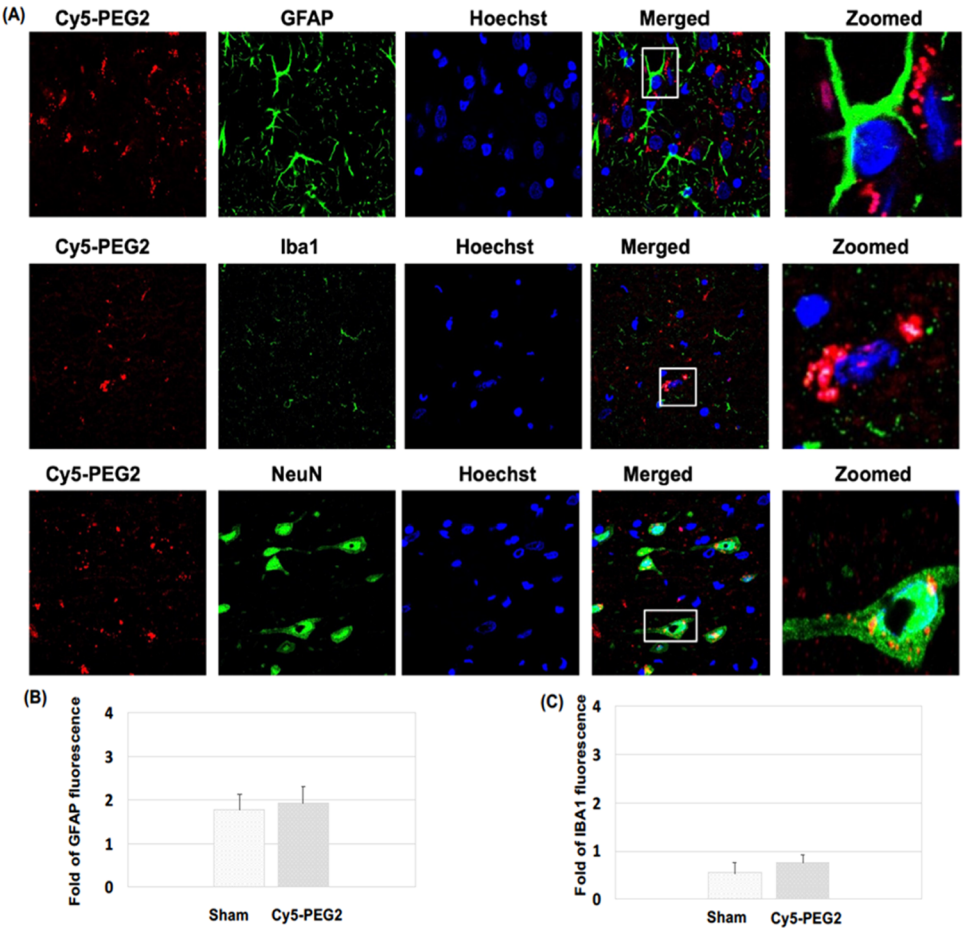

Figure 6. Visualization of the Cy5-PEG2 dye in the neocortex regions: (A) representative confocal laser scanning images of rat brain sections fixed with 4% PFA. For the entire figure, the red channels represent the fluorescent dye Cy5-PEG2; the green channel represents GFAP- (row I), Iba1- (row II), and NeuN-positive (row III) cells in the brain sections. Zoomed-in pictures are shown on the right. The fluorescent images were obtained with a confocal laser scanning fluorescent microscope using a 60 × objective lens. (B) Quantitative analysis of the fluorescence intensity of GFAP. (C) Quantitative analysis of the fluorescence intensity of IBA1.

undergoes degradation or photobleaching over time, decreasing the staining intensity.

The permeability of the blood−brain barrier may change over time. Initially, the peptide could be more permeable, allowing a higher concentration of Cy5 derivatives to enter the brain. However, this permeability may decrease over 24 h. Conversely, the presence of CY5-PEG2 in the brain may trigger an inflammatory or immune response, which could lead to clearance or altered distribution of the dye over time.

We need to conduct further experiments and analyses to understand better the specific reason for the observed change in the staining intensity. This could involve investigating the metabolism of Cy5-PEG2, monitoring their distribution in different brain regions, and assessing any potential toxic or immune responses that might affect their presence in the brain over time. Additionally, considering the specific properties of Cy5-PEG2 and their interactions with biological systems would be crucial for a more accurate explanation. Our team is conducting systematic studies of the biodistribution and pharmacokinetics of this imaging agent and will promptly report the results.

3.6. Intraperitoneal Administration of Cy5-PEG2 Dye in SD Rats: Absence of Glial Activation and Inflammatory Responses. GFAP and IBA1 are biomarkers commonly used to assess the activation and response of glial cells in the central nervous system. Following brain injury or neurodegenerative conditions, the level of GFAP expression increases. This upregulation is known as astrogliosis, a typical response to neuronal damage or inflammation in the brain.[10] Monitoring GFAP levels can provide insights into the degree of glial activation and the extent of neural injury or damage caused by injected agents such as Cy5-PEG2. Elevated GFAP expression may indicate a toxic response or neuroinflammation.

Iba1 is a protein only in microglia, immune cells in the central nervous system. Microglia play an essential role in the brain's immune response by detecting and monitoring pathogens, damaged neurons, and abnormal protein clusters. Microglia change their appearance and increase their Iba1 expression when activated, indicating their immune response and inflammation involvement.[10] Tracking Iba1 levels can evaluate microglial activation and neuroinflammation after injecting substances like Cy5-PEG2. An increase in Iba1 expression may suggest a potential toxic or inflammatory response (Figures 5 and 6).

By quantifying the levels of GFAP and Iba1 expressions, we could assess the potential toxicity of the Cy5-PEG2 dye when intraperitoneal injection was administered to SD rats (Figures 5B,C and 6B,C). Our results indicate no significant increases in GFAP and Iba1 levels, which suggests that the Cy5-PEG2 dye

https://doi.org/10.1021/acsomega.3c07374
ACS Omega 2024, 9, 2585−2596

did not cause glial activation or inflammatory responses. Furthermore, there were no observable negative consequences or neurotoxicity to the central nervous system.

4. DISCUSSION

Live-cell imaging using fluorescent dyes such as MitoTracker can help visualize mitochondria in various cell types. However, using these dyes for in vivo brain cell imaging is challenging due to specific limitations. For example, MitoTracker dyes need to penetrate plasma and mitochondrial membranes to label mitochondria, which is difficult in brain imaging due to the BBB, which affects their effectiveness in penetrating brain cells. Additionally, imaging deep brain regions can be challenging due to light scattering, absorption, and tissue autofluorescence, which can disrupt clear and specific labeling with MitoTracker dyes. Lastly, MitoTracker dyes can sometimes accumulate in other cellular compartments or structures, leading to potential false signals or confusion in interpretation.[11] To overcome these limitations, we aim to find new fluorescent dyes that target mitochondria and aid in studying these organelles, particularly for in vivo brain imaging.

Developing new fluorescent dyes that specifically target mitochondria in brain cells in vivo is a complex and challenging process. Brain cells have unique characteristics that pose specific obstacles such as mitochondrial specificity, BBB penetration, photostability and brightness, biocompatibility, mitochondrial dynamics and morphology, long-term imaging and live-cell applications, and background fluorescence and autofluorescence.

Cyanine dyes are highly beneficial in bioimaging due to their distinct optical properties.[3,7] They possess strong fluorescence, high quantum yields, and good photostability, making them ideal for various imaging techniques. By fluorescently labeling biomolecules such as proteins, nucleic acids, and lipids, cyanine dyes allow for easy visualization and tracking of these molecules within living cells and tissues. In microscopy, researchers commonly use cyanine dyes as fluorescent probes to study cellular structures and dynamics with high resolution and sensitivity. Additionally, these dyes serve as optical imaging probes for specific applications, providing valuable insights into cellular processes and pathological conditions. Overall, cyanine dyes are excellent tools for bioimaging with several practical applications in the field. Based on these positive results, we have created a range of new fluorescent dyes using cyanine for imaging mitochondria. This work details the development, synthesis, and testing of one of these new fluorescent dyes, Cy5-PEG2, which can be used for both in vitro and in vivo imaging of brain cell mitochondria.

AD patients often have neurofibrillary tangles and senile plaque in their brains. Senile plaque is made up of Aβ peptides, while neurofibrillary tangles are comprised of hyperphosphorylated tau protein.[9] The neocortex is typically the first area of the brain to display senile plaques, followed by the hippocampus and the rest of the brain in a centripetal pattern. The accumulation of Aβ peptides within the cells leads to this damage. Amyloid precursor protein (APP), a transmembrane protein expressed on chromosome 21 in neuronal synapses, is critical for neuronal development. Aβ peptides are an abnormal proteolytic byproduct of APP.[12] In a healthy brain, APP undergoes alternative splicing, cleaving by α-secretase at or near lysine-16 in the Ab sequence on neuron surfaces.[12] This releases the C-terminal site of soluble APP-α from the membrane and subsequent secretion, reducing the level of Aβ protein deposition in cells. However, in the case of AD, APP is cleaved by β- and γ-secretase, leading to the formation of several isoforms of Aβ peptides ranging in length from 39 to 43 residues.[12] Aβ fibrils found in senile plaques are usually the Aβ species that end at amino acid 42 (Aβ42). These fibrils are longer and more hydrophobic than the other Aβ species, making them more prone to aggregation and toxicity.

Previous studies suggested that accumulating Aβ peptides in the brain can have severe consequences.[12,13] It can trigger the production of reactive oxygen species (ROS), initiate cell death processes, and increase neurotoxicity. Aβ peptides have been identified as the cause of dendritic degeneration and loss of synapses, which ultimately leads to neuronal death in the rat hippocampus.[12] Additionally, in vitro studies using cells from PC12 cells (rat pheochromocytoma[14,15] and SH-SY5Y cells)[16,17] (human neuroblastoma) have demonstrated that extracellular fibrillar aggregates of Aβ peptides are neurotoxic. However, these cells are unsuitable for neurodegenerative disease research due to their instability and inability to create a diverse population of neurons.

Our present study utilized primary neuronal cells derived directly from the nervous system to understand how Aβ peptide affects mitochondrial morphology and dynamics. These cells are a biologically relevant model that closely mimics the brain's cellular environment, making it easier to study the molecular mechanisms underlying AD. To evaluate this effect, we used the Cy5-PEG2 dye to monitor the alterations in the mitochondrial morphology and function of primary neuron cells.

Mitochondria are essential organelles known as the "powerhouses" of the cell because they produce energy through oxidative phosphorylation, which generates ATP. They also play a crucial role in other cellular processes, such as apoptosis, calcium homeostasis, and cellular signaling. Mitochondria are dynamic organelles that can undergo fusion and fission processes, contributing to the maintenance of mitochondrial function and overall cellular health.

Our present study examined the effects of the Aβ_{1-42} peptide on mitochondrial morphology and dynamics. The Aβ_{1-42} peptide can increase the number of fragmented mitochondria at high concentrations. This process may result from increased cellular stress or damage. Mitochondria fission can lead to mitochondria fragmentation, impairing their function and ultimately contributing to cellular dysfunction. Interestingly, the Aβ_{1-42} peptide was observed to increase the percentage of elongated mitochondria at low concentrations. Mitochondrial fusion might be an adaptive response to cellular stress, possibly aimed at improving mitochondrial function by sharing resources and repairing damaged mitochondria.

AD is characterized by the accumulation of amyloid β peptides in the brain, forming plaques and subsequent neurodegeneration. Interestingly, depending on concentration, the Aβ_{1-42} peptide can affect mitochondrial morphology and dynamics. One significant finding is that high concentrations of the Aβ_{1-42} peptide can cause mitochondria fission, which is the splitting of mitochondria into smaller units. Fission can lead to various cellular stress responses, energy imbalances, and cell death when fission is not regulated correctly. This is particularly relevant to AD, as disrupted mitochondrial dynamics can contribute to neuronal dysfunction and degeneration.[13] On the other hand, low concentrations of the Aβ_{1-42} peptide can induce mitochondria fusion, which is the merging of mitochondria. This process helps maintain

https://doi.org/10.1021/acsomega.3c07374
ACS Omega 2024, 9, 2585−2596

mitochondrial function and cellular health by redistributing mitochondrial components, sharing mitochondrial DNA, and rescuing damaged mitochondria.

The findings in our present study suggest that modulating mitochondrial dynamics could be a potential strategy to counteract the adverse effects of the Aβ peptide. By promoting fusion or inhibiting excessive fusion, we may be able to mitigate the impact of high Aβ_{1-42} concentrations or prevent the accumulation of dysfunctional mitochondria. It is important to note that the effects of Aβ_{1-42} on mitochondria are concentration-dependent. This highlights the complex and often biphasic nature of cellular responses to pathological factors. Therefore, studying dose−response relationships is crucial when investigating the impact of such molecules on cellular processes. These findings also underscore how the Aβ_{1-42} peptide can induce cellular stress responses that contribute to disease progression. Dysregulation of mitochondrial dynamics is not limited to AD but is a common theme in various neurodegenerative disorders, including Parkinson's and Huntington's.[2,13] These observations provide valuable insights into the intricate relationship between amyloid β peptide and mitochondrial dynamics. Further research in this area may lead to potential therapeutic strategies to counteract the detrimental effects of the amyloid β peptide on mitochondrial function and neuronal health.

Our investigation into the toxicity profile of Cy5-PEG2 dye in the brain involved carefully examining its impact on glial activation, neuronal health, and potential neuroinflammation. After conducting our study, we did not identify any significantly increased levels of GFAP and Iba1, indicating that the injected Cy5-PEG2 did not trigger glial activation or inflammatory responses. Moving forward, assessing changes in neuronal morphology, synaptic integrity, and cell viability would be beneficial to gain a more comprehensive understanding of this dye's toxicity profile.

5. CONCLUSIONS

A new fluorescent dye, Cy5-PEG2, has been developed to accumulate in mitochondria, enabling in vivo brain imaging. This advancement is significant, as it can penetrate the BBB, making it an excellent tool for monitoring mitochondrial dynamics in living cells. It is expected to be used to study mitochondrial dynamics and function in the context of whole-brain physiology and disease progression.

6. LIMITATIONS

Based on the data we have collected thus far, the Cy5-PEG2 dye we administered does not significantly impact the expression levels of GFAP and Iba1 in brain tissues. This suggests that the dye does not activate glial cells or cause neuroinflammation. Furthermore, we did not detect any toxicities in the markers we analyzed. However, it may be beneficial to investigate other markers of inflammation or neurotoxicity to achieve a more comprehensive evaluation of this dye.

AUTHOR INFORMATION

Corresponding Authors

Zhiying Shan − *Department of Kinesiology and Integrative Physiology and Health Research Institute, Michigan Technological University, Houghton, Michigan 49931, United States;* orcid.org/0000-0002-9763-205X; Email: zhiyings@mtu.edu

Lanrong Bi − *Department of Chemistry, Michigan Technological University, Houghton, Michigan 49931, United States; Health Research Institute, Michigan Technological University, Houghton, Michigan 49931, United States;* orcid.org/0000-0001-6624-8314; Email: lanrong@mtu.edu

Authors

Xin Yan − *Department of Chemistry, Michigan Technological University, Houghton, Michigan 49931, United States; Health Research Institute, Michigan Technological University, Houghton, Michigan 49931, United States*

Xinqian Chen − *Department of Kinesiology and Integrative Physiology and Health Research Institute, Michigan Technological University, Houghton, Michigan 49931, United States*

Complete contact information is available at: https://pubs.acs.org/10.1021/acsomega.3c07374

Notes

The authors declare no competing financial interest.

ACKNOWLEDGMENTS

This project was partially supported by AHA 1807047 (Bi), GLRC-ICC (R01805), NIHR15HL150703 (Shan), and NIHR01HL163159 (Shan). The authors thank Dr. Rick Koubek for fostering a supportive environment for our ongoing projects.

REFERENCES

(1) Mantle, D.; Hargreaves, I. P. Mitochondrial Dysfunction and Neurodegenerative Disorders: Role of Nutritional Supplementation. *Int. J. Mol. Sci.* **2022**, *23* (20), 12603 DOI: 10.3390/ijms232012603. PMID: 36293457; PMCID: PMC9604531.

(2) Guo, J.; Huang, X.; Dou, L.; Yan, M.; Shen, T.; Tang, W.; Li, J. Aging and aging-related diseases: from molecular mechanisms to interventions and treatments. *Signal Transduction Targeted Ther.* **2022**, *7* (1), 391 DOI: 10.1038/s41392-022-01251-0. PMID: 36522308; PMCID: PMC9755275.

(3) Qiu, Y.; Yuan, B.; Cao, Y.; He, X.; Akakuru, O. U.; Lu, L.; Chen, N.; Xu, M.; Wu, A.; Li, J. Recent progress on near-infrared fluorescence heptamethine cyanine dye-based molecules and nanoparticles for tumor imaging and treatment. *Wiley Interdiscip. Rev.: Nanomed. Nanobiotechnol.* **2023**, *15*, No. e1910, DOI: 10.1002/wnan.1910. Epub ahead of print. PMID: 37305979.

(4) Teunissen, C. E.; Verberk, I. M. W.; Thijssen, E. H.; Vermunt, L.; Hansson, O.; Zetterberg, H.; van der Flier, W. M.; Mielke, M. M.; Del Campo, M. Blood-based biomarkers for Alzheimer's disease: towards clinical implementation. *Lancet Neurol.* **2022**, *21* (1), 66−77 Jan. Epub 2021 Nov 24. PMID: 34838239.

(5) Gallardo, G.; Holtzman, D. M. Amyloid-β and Tau at the Crossroads of Alzheimer's Disease. *Adv. Exp. Med. Biol.* **2019**, *1184*, 187−203. PMID: 32096039.

(6) Jeremic, D.; Jiménez-Díaz, L.; Navarro-López, J. D. Past, present and future of therapeutic strategies against amyloid-β peptides in Alzheimer's disease: a systematic review. *Ageing Res. Rev.* **2021**, *72*, No. 101496. Dec Epub 2021 Oct 21. PMID: 34687956.

(7) Ilina, K.; Henary, M. Cyanine Dyes Containing Quinoline Moieties: History, Synthesis, Optical Properties, and Applications. *Chem. - Eur. J.* **2021**, *27* (13), 4230−4248 Mar 1 DOI: 10.1002/chem.202003697. Epub 2020 Dec 29. Erratum in: Chemistry. 2022 Apr 22;28(23):e202104530. PMID: 33137212; PMCID: PMC9832344.

(8) Turecek, P. L.; Bossard, M. J.; Schoetens, F.; Ivens, I. A. PEGylation of Biopharmaceuticals: A Review of Chemistry and Nonclinical Safety Information of Approved Drugs. *J. Pharm. Sci.* **2016**, *105* (2), 460−475. PMID: 26869412.
(9) Busche, M. A.; Hyman, B. T. Synergy between amyloid-β and tau in Alzheimer's disease. *Nat. Neurosci.* **2020**, *23* (10), 1183−1193. Epub 2020 Aug 10. PMID: 32778792.
(10) Novoa, C.; Salazar, P.; Cisternas, P.; Gherardelli, C.; Vera-Salazar, R.; Zolezzi, J. M.; Inestrosa, N. C. Inflammation context in Alzheimer's disease, a relationship intricate to define. *Biol. Res.* **2022**, *55* (1), 39 DOI: 10.1186/s40659-022-00404-3. PMID: 36550479; PMCID: PMC9784299.
(11) Kilgore, J. A.; Dolman, N. J. A Review of Reagents for Fluorescence Microscopy of Cellular Compartments and Structures, Part II: Reagents for Non-Vesicular Organelles. *Curr. Protoc.* **2023**, *3* (6), No. e752, DOI: 10.1002/cpz1.752. Jun PMID: 37310209.
(12) Gouras, G. K.; Olsson, T. T.; Hansson, O. β-Amyloid peptides and amyloid plaques in Alzheimer's disease. *Neurotherapeutics* **2015**, *12* (1), 3−11, DOI: 10.1007/s13311-014-0313-y. PMID: 25371168; PMCID: PMC4322079.
(13) Rai, S. N.; Singh, C.; Singh, A.; Singh, M. P.; Singh, B. K. Mitochondrial Dysfunction: a Potential Therapeutic Target to Treat Alzheimer's Disease. *Mol. Neurobiol.* **2020**, *57* (7), 3075−3088, DOI: 10.1007/s12035-020-01945-y. Epub 2020 May 27. PMID: 32462551.
(14) Stańczykiewicz, B.; Goszczyński, T. M.; Migdał, P.; Piksa, M.; Pawlik, K.; Gburek, J.; Gołąb, K.; Konopska, B.; Zabłocka, A. Effect of Ovocystatin on Amyloid β 1−42 Aggregation-In Vitro Studies. *Int. J. Mol. Sci.* **2023**, *24* (6), 5433 DOI: 10.3390/ijms24065433. PMID: 36982505; PMCID: PMC10049317.
(15) Sánchez, Y.; Castillo, C.; Fuentealba, J.; Sáez-Orellana, F.; Burgos, C. F.; López, J. J.; F de la Torre, A.; Jiménez, C. A. New Benzodihydrofuran Derivatives Alter the Amyloid β Peptide Aggregation: Strategies To Develop New Anti-Alzheimer Drugs. *ACS Chem. Neurosci.* **2023**, *14* (15), 2590−2602, DOI: 10.1021/acschemneuro.2c00778. Epub 2023 Jul 22. PMID: 37480555.
(16) Samandari-Bahraseman, M. R.; Elyasi, L. Apelin-13 protects human neuroblastoma SH-SY5Y cells against amyloid-beta induced neurotoxicity: Involvement of anti oxidant and anti apoptotic properties. *J. Basic Clin. Physiol. Pharmacol.* **2022**, *33* (5), 599−605, DOI: 10.1515/jbcpp-2020-0294. PMID: 33977683.
(17) Kola, A.; Lamponi, S.; Currò, F.; Valensin, D. A Comparative Study between Lycorine and Galantamine Abilities to Interact with AMYLOID β and Reduce In Vitro Neurotoxicity. *Int. J. Mol. Sci.* **2023**, *24* (3), 2500 DOI: 10.3390/ijms24032500. PMID: 36768823; PMCID: PMC9916559.

https://doi.org/10.1021/acsomega.3c07374
ACS Omega 2024, 9, 2585−2596